Adhesion of tungsten particles on rough tungsten surfaces using Atomic Force Microscopy

Samuel Peillon, Adrien Autricque, Michaël Redolfi, Cristian Stancu, François Gensdarmes, Christian Grisolia, Olivier Pluchery

Samuel Peillon, Adrien Autricque, Michaël Redolfi, Cristian Stancu, François Gensdarmes, et al.. Adhesion of tungsten particles on rough tungsten surfaces using Atomic Force Microscopy. Journal of Aerosol Science, 2019, 137, pp.105431. 10.1016/j.jaerosci.2019.105431 . hal-02322543

Adhesion of tungsten particles on rough tungsten surfaces using Atomic Force Microscopy

Samuel Peillon[a,e], Adrien Autricque[b], Michaël Redolfi[c], Cristian Stancu[d], François Gensdarmes[a], Christian Grisolia[b], Olivier Pluchery[e]

[a]*Institut de Radioprotection et de Sûreté Nucléaire (IRSN), PSN-RES/SCA, BP 68, 91192 Gif-sur-Yvette, France*
[b]*CEA, IRFM, F-13108 Saint Paul lez Durance, France*
[c]*LSPM, CNRS-UPR3407, Université Paris 13 Sorbonne Paris Cité, 99 Avenue J. B. Clément, 93430 Villetaneuse, France*
[d]*National Institute for Lasers, Plasma and Radiation Physics, Magurele, 077125, Romania*
[e]*Sorbonne Universités, UPMC-CNRS, Institut des Nanosciences de Paris, 4 place Jussieu, 75252 Paris, Cedex 05, France*

Abstract

Adhesion forces between tungsten spherical microparticles and tungsten substrates with different roughnesses have been measured using the Atomic Force Microscopy (AFM) colloidal probe technique. Mean roughnesses of the tungsten substrates were measured by AFM and were ranked in three categories i.e. nanoscale, sub-microscale and microscale roughnesses. Experimental Hamaker constant of $37 \pm 3.5 \times 10^{-20}$ J has been obtained using a spherical tungsten particle of 10.5 μm in radius and a tungsten substrate with nanoscale root-mean-square roughness of rms = 11.5 nm. It was shown that larger roughness of the order rms = 712 nm induces a two order of magnitude decrease on the adhesion of tungsten microparticles compared to a smooth tungsten surface with nanoscale roughness. Comparison with the van der Waals-based adhesion force model of Rabinovich which integrates the roughness of surfaces showed good agreement with experimental pull-off forces even when roughness of the substrate is close to the micrometer range. In such case, measurements have shown that dependency of adhesion force with particle size (in the micrometer range) has a secondary influence compared to the roughness of surfaces.

Keywords: Adhesion, Roughness, Tungsten, Hamaker constant, Atomic Force Microscopy

---

Introduction

The study of adhesion of microparticles on surfaces have numerous applications in many different fields of research. It is, for example, particularly of great importance in the evaluation of resuspension or removal of particulate contaminants from rough surfaces encountered in domains such as biotechnology, micro and nanoelectronic or powder handling in pharmaceutic or nuclear industry. In this latter domain, special attention to the safety and operation of next-generation nuclear fusion facilities has emerged over the years. Indeed, large amount of metallic dusts (Krasheninnikov et al. [2011]) will be generated by energetic plasma-surface interactions that cause significant erosion of the vacuum vessel (VV) plasma facing-components (PFCs) made from beryllium and tungsten. Characterization

---

Email address: `samuel.peillon@irsn.fr` (Samuel Peillon) of the behavior of these dusts and especially the amount of particles that can be re-suspended or are already airborne during normal operations is of primary interest for the design and the definition of the functioning procedure and safety domain of these facilities. Therefore, it is necessary to know *a priori* the adhesive properties of these particles on specific surfaces of interest such as rough tungsten or beryllium to evaluate their re-suspension potential. Despite its importance, the phenomenon of adhesion of particles on rough surfaces is difficult to measure in a quantitative way because of its complexity. For example, environmental conditions (humidity, temperature), geometry (size, roughness) of the surfaces in contact, energetic heterogeneity and chemical interactions can influence the adhesion force. In particular, value of adhesion energy for tungsten surfaces is still poorly documented and recent studies (Rondeau et al. [2015], Peillon et al. [2017], Tolias et al. [2018]) are questioning data found in the literature for this material. Detachment of microparticles from rough substrates is a process resulting from the competition between the removal force e.g. aerodynamic, electrostatic, centrifuge or inertial and the particle-surface interactions among them adhesive forces. In the case where a large number of microparticles are dispersed on a surface, the strength necessary to detached each particles will not be constant and is usually approximated by a log-normal distribution. It is customary to determine experimentally the adhesion force by calculating the ratio between the number of particles detached by a certain force and the number of particles initially deposited on the surface. There are many methods for measuring adhesion strength between particles and surfaces. One common method is centrifugation (Krupp [1967], Mizes et al. [2000], Salazar-Banda et al. [2007], Petean and Aguiar [2015]), where particles are being detached by centrifugal forces when the surface on which they are deposited is rotated rapidly. Aerodynamic detachment method (Matsusaka and Masuda [1996], Peillon et al. [2014], Brambilla et al. [2017]), vibration method (Ripperger and Hein [2004]), or inertial detachment (Wanka et al. [2013], Zafar et al. [2014]) have also been proposed to measure the adhesion force distribution of a set of particles deposited on a substrate. Other known methods like electrostatic detachment based on planar capacitor devices in which particles are exposed to increasing electric fields have been used extensively (Cho [1964], Cooper et al. [1988], Takeuchi [2006], Szarek and Dunn [2007]). Very recently this method has been employed specifically for tungsten spherical particles deposited on tungsten substrates with the aim of determining detachment correlation between particle diameter and electric field detachment threshold (Riva et al. [2017], Peillon et al. [2017], Tolias et al. [2018]). Such techniques make it possible to obtain the distribution of the adhesion forces for a large number of particles, thus with a good statistical representation. However, some common drawbacks such as control of the electric charge on the particles, uniformity of the electric fields, particle shape and spread of particle size distribution bring certain limitations for quantitative adhesion studies.

On the other hand, the colloidal probe technique introduced by Ducker et al. [1991] permits the measurement of the total adhesion force (or pull-off force) between a single particle and a substrate. Over the years, Atomic Force Microscopy (AFM) became a reliable method to confront adhesion theoretical models with quantitative measurements of adhesion forces (Butt et al. [2005], Leite et al. [2012]). Indeed, contact mechanic models such as JKR (Johnson et al. [1971]), DMT (Derjaguin et al. [1975]) or Maugis - Dugdale (M-D) (Maugis [1992]) as well as van der Waals based model (Hamaker [1937], Parsegian [2005]) have been consistently tested by means of AFM force spectroscopy technique with common materials such as silica (Olsson et al. [1992], Jones et al. [2002]), alumina (Götzinger and Peukert [2003]), polystyrene (Gauthier et al. [2013]) copper (Butt et al. [2005]), gold (Heim et al. [2002]) or stainless steel (Götzinger and Peukert [2004]). Nevertheless, only few work have been initiated to evaluate the adhesion force with AFM technique between relevant dusts and surfaces one can find in nuclear fusion facilities. To our knowledge, only few studies (Mokgalapa et al. [2014], Zhang et al. [2015]) between graphene particles with complex geometry and different types of surfaces found in High Temperature Reactors (HTR) have been performed so far with AFM. However, in both aforementioned studies, roughness of surfaces and irregularity of particles were not controlled which makes the comparison with adhesion models difficult. Reduction of adhesion by roughness of surfaces is a well-documented topic since Fuller and Tabor [1975] conducted systematic studies of roughness effect on the adhesion and suggested taking into account the distribution of heights of substrates in the calculation of adhesive forces. Further developments based on the Hamaker theory (Hamaker [1937]) were proposed by Rumpf [1990] and later by Rabinovich et al. [2000b] by considering asperities on the surface as protruding hemispheres or submerged spheres for the latter. In these van der Waals based theories, surface deformation is not considered contrary to the mechanic theories of adhesion of JKR/DMT models that take into account the surface of the contact area between the two bodies under specific external load and the surface energy of adhesion to determine the pull-off force. When applied to rough surfaces, these smooth-surface models have shown to greatly over-estimate the adhesion force (Götzinger and Peukert [2003]).

In this paper, we focus on direct measurement of adhesion force (or pull-off force) between hard spherical tungsten particles with sizes in the micrometer range and tungsten surfaces with various roughness using Atomic Force Microscopy (AFM). The spherical shape of particles is a prerequisite for proper comparison between adhesion force models and pull-off force experiments. In the first part of this manuscript, van der Waals based theory of adhesion with the integration of roughness effect will be introduced and domains of applicability of the theory will be discussed. The second part of the present paper will address the experimental method implemented for the pull-off force measurements. A special attention has been given to the production of samples with defined shapes and roughness and the characterization of contacting surfaces during experiments. A wide range of spherical tungsten particles were produced and studied from 1 μm to 10.5 μm in radius. Likewise, tungsten substrates with three different scales of roughness were fabricated and analyzed with AFM. In the third part of the paper, results of pull-off force measurements will be presented and a comparison with van der Waals based force models of Rumpf [1990] and Rabinovich et al. [2000a] is proposed. Estimation of the Hamaker constant for W/W interaction in ambient air is also addressed in this section.

1. Theoretical considerations

General adhesion of solids is governed by various phenomena such as capillary forces in the presence of water vapor, electrostatic forces when particles possess electrical charges (friction, radioactivity), hydrogen bonds in case of chemical reactive surfaces and van der Waals forces. In the present study, capillary forces are not discussed and are considered as non determinant parameters since measurements were taken at a constant humidity level of 40 %. As the study is focused on the adhesion of similar materials (tungsten) and as grafted particles were actually used a long time after their fabrication, electrostatic interactions can also be neglected and the following will focus on the influence of surface roughness on the adhesion.

1.1. The Hamaker theory

The Hamaker [1937] theory describes interactions between pairs of atoms composing non-deformable macroscopic objects. These atom-atom interactions are additive and ruled by the Hamaker constant and the distance between objects. The van der Waals force between a smooth sphere and a smooth planar surface is expressed by the Hamaker theory,

$$F_{vdW} = \frac{A \cdot R_p}{6 \cdot z_0^2}, \tag{1}$$

with A the Hamaker constant, R_p the particle radius and z_0 the distance of closest approach between surfaces. In this theory, surfaces in contact are perfectly smooth which leads to consider the closest distance between materials z_0 as the intermolecular length scale generally around 0.4 nm (Israelachvili [2011]). An early model that integrates roughness effect to Hamaker theory by changing the geometry of the problem was introduced by Rumpf [1990].

1.2. The Rumpf theory

The Rumpf model consists of two terms that describe the total van der Waals interaction between a large spherical particle and hemispherical asperity protruding a plane surface as depicted in Figure 1. The first term represents direct interaction (contact) between the particle and the asperity while the second term stands for "non-contact" interactions between the particle and the surface separated by the height of the asperity. The corresponding van der Waals force is written as follows:

$$F_{vdW} = \frac{A}{6 \cdot z_0^2}\left[\frac{r_s \cdot R_p}{r_s + R_p} + \frac{R_p}{(1 + r_s/z_0)^2}\right] \tag{2}$$

with r_s the asperity radius. Rabinovich et al. [2000b] pointed out that with such a geometry, the center of the hemispherical asperity must be located at the surface which is generally too much simplification for real substrate.

In addition, Rabinovich noted that the radius of asperity is difficult to measure while common AFM technique is able to measure accurately the height and root-mean-square (*rms*) roughness of surfaces. Hence, Rabinovich *et al.* proposed a relationship between the radius of asperity and *rms* roughness defined as follows:

$$r_s = 1.485 \cdot rms. \tag{3}$$

Substituting (3) in (2) leads to the following expression:

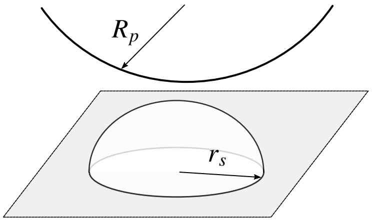

Figure 1: Schematic illustration of the geometry proposed by Rumpf for the interaction of a spherical particle with radius R_p with an hemispherical asperity of radius r_s.

$$F_{vdW} = \frac{A \cdot R_p}{6 \cdot z_0^2} \left[\frac{1}{1 + R_p/(1.485 \cdot rms)} + \frac{1}{(1 + 1.485 \cdot rms/z_0)^2} \right], \tag{4}$$

which is referred to by Rabinovich et al. [2000b] as the modified Rumpf's model . When more than one scale roughness is considered, the global equivalent roughness of the surface can be calculated as follows:

$$rms = \sqrt{rms_1^2 + rms_2^2}, \tag{5}$$

where rms_1 and rms_2 are the average root-mean-square roughnesses of the long and short peak-to-peak distances respectively (Rabinovich et al. [2000a]). Figure 2 depicts the evolution of total adhesion forces normalized by the radius of the particle using the relation (4) for tungsten particles with radius $R_p = 2.5$ μm, 5 μm and 10 μm, Hamaker constant for pure W/W interaction $A = 49 \cdot 10^{-20}$ J given by Tolias [2018] and closest distance approach between surfaces $z_0 = 0.45$ nm (Israelachvili [2011]). Total adhesion force exhibits two distinct regimes depending on the surface roughness at the nanoscale. For a *rms* roughness above 10 nm, the normalized adhesion is ruled by the contact term of the modified Rumpf equation whereas the non-contact interaction between the particle and the surface dominates for *rms* roughness below 10 nm. As pointed out by Xie [1997], surfaces with such small *rms* roughness (below 10 nm) will be treated as smooth. As depicted by Figure 2, in the non-contact interaction regime corresponding to nanoscale roughness below 10 nm, the normalized adhesion force is independent on the particle radius (second term in Eq. 4) and increases when nanoscale roughness decreases. However this observation is not valid for the contact adhesion force regime (first term in Eq. 4) where the normalized force decreases as the particle's size increases for a given *rms* roughness. Indeed, as the particle's radius increases, the minimum normalized adhesion force decreases and a shift in the contact component towards higher *rms* roughness occurs. This prediction of the modified Rumpf model for roughnesses above tens of nanometers has been discussed extensively in the literature (Götzinger and Peukert [2003], Laitinen et al. [2013], LaMarche et al. [2017]) and systematically shows poor agreement with experiment underestimating the adhesion force.

1.3. The Rabinovich model

The poor agreement between the Rumpf theory and experiment for large nanoscale roughness has conducted Rabinovich et al. [2000b] to further develop the surface geometry by considering that the center of the hemispherical

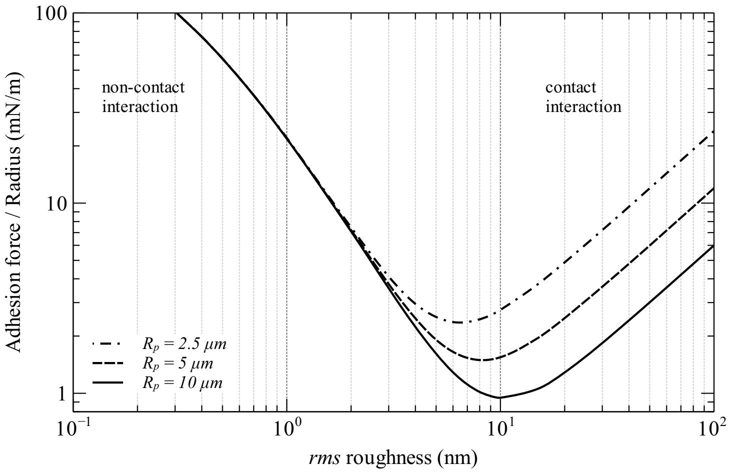

Figure 2: Total adhesion force normalized by the particle radius (R_p = 2.5 μm, 5 μm and 10 μm) using the modified Rumpf model (4) with Hamaker constant of $49 \cdot 10^{-20}$ J (Tolias [2018]) and distance of closest approach z_0 = 0.45 nm.

asperity is generally not aligned with the surface but embedded below it. In addition to the height of asperities, a new parameter λ referred to as the breadth between asperities has been added to the model.

Moreover, authors observed that common surfaces are always composed of a nanoscale roughness superimposed on a larger microscale roughness (also referred to as waviness) with much longer peak-to-peak distance. Rabinovich *et al.* thus incorporated the contribution of two scales of surface roughness, characterized by their root-mean-square roughness rms_i and peak-to-peak distances λ_i. The total adhesion force is simply the sum of the contribution of the adhesion of the particle with the different roughness structures and the underlying plane and is given by Rabinovich et al. [2000b]:

$$F_a = \frac{A \cdot R_p}{6 \cdot z_0^2}\left[\frac{1}{1 + 58\mathrm{rms}_2 R_p/\lambda_2^2} + \frac{1}{\left(1 + 58\mathrm{rms}_1 R_p/\lambda_1^2\right)(1 + 1.82\mathrm{rms}_2/z_0)^2} + \frac{z_0^2}{(1 + 1.82\,(\mathrm{rms}_1 + \mathrm{rms}_2))^2}\right]. \qquad (6)$$

Figure 3 depicts such a geometry considering two superimposed roughness as described by Rabinovich. Note that for this geometry, the height of the asperity above the average surface plane is not equal to the radius of the asperity and its origin is located below the average surface plane.

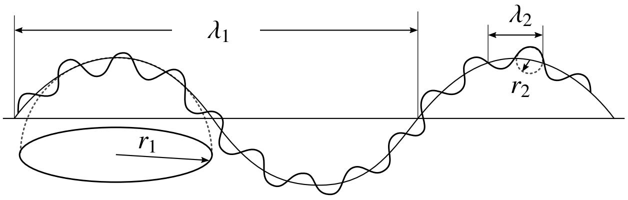

Figure 3: Schematic illustration of the geometry proposed by Rabinovich *et al.* for the interaction of a spherical particle with a surface composed of two scales of roughness.

Eq. (6) is valid as long as the *rms* and wavelength of the two scales roughness remain smaller than the size of the adhering particle. When λ_1 becomes comparable to R_p, the average plane of the surface is incorporated in the large asperities and the third term of eq. (6) can be dropped, yielding:

$$F_a = \frac{A \cdot R_p}{6 \cdot z_0^2} \left[\frac{1}{1 + 58\text{rms}_2 R_p/\lambda_2^2} + \frac{1}{\left(1 + 58\text{rms}_1 R_p/\lambda_1^2\right)(1 + 1.82\text{rms}_2/z_0)^2} \right]. \tag{7}$$

In such a case ($\lambda_1 > R_p$), the contact term provides the major contribution to the total adhesion force although the non-contact term keeps its influence in the nanoscale roughness regime. This situation is depicted in Figure 4 representing the total adhesion force normalized by the particle radius according to the superimposed roughness (rms_2) while other surface parameters are kept constant. The Hamaker constant and distance of closest approach are identical to the example in Figure 2.

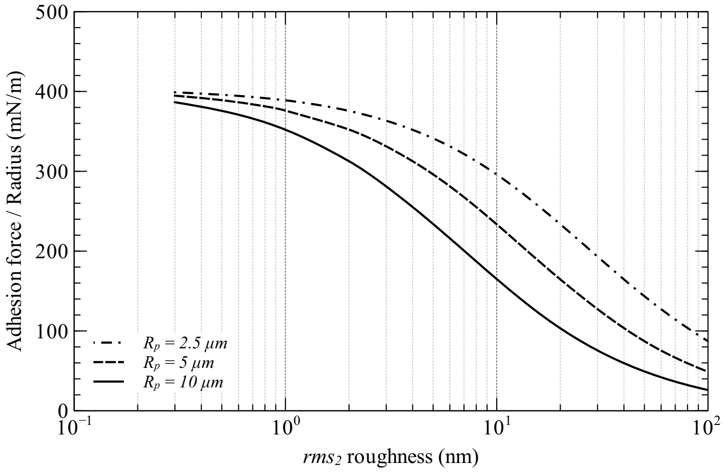

Figure 4: Total adhesion force normalized by the particle radius ($R_p = 2.5\ \mu$m, 5 μm and 10 μm) using the Rabinovich model with the same parameters of Figure 2 (Hamaker constant of $49 \cdot 10^{-20}$ J and distance of closest approach $z_0 = 0.45$ nm).

In contrast with the modified Rumpf model, the Rabinovich model does not predict a minimum value for the total normalized adhesion force but a continuous decrease with the increase of the superimposed roughness of the surface. This eliminates the increase in the normalized adhesion force predicted by the modified Rumpf model for *rms* roughnesses above 10 nm previously described in Figure 2. Moreover, values of normalized adhesion forces appear to be a full order of magnitude greater than calculated with the modified Rumpf model. Although the geometry proposed by Rabinovich shows good results when compared to experiments (Laitinen et al. [2013]), it has some limitations: (i) particles and surfaces that come in contact are regarded as nondeformable under the applied loads. Plastic deformation is thus neglected; (ii) it considers a single point of contact between the particle and the surface which can be different from the equilibrium position. Nevertheless, when using the colloidal AFM technique, particles are fixed under the cantilever and thus not free to move to find more than one contact point. In addition, the use of a hard material such as tungsten (Young's modulus of $E = 400$ GPa at room temperature) for both the particle and the surface material reduces to its minimum the plastic deformations that can arise during contact.

2. Experimental methods

2.1. Adhesion force measurements

Adhesion force measurements have been realized with a Multimode 8 (Bruker™) AFM in PeakForce Quantitative Nano-Mechanical mode (PF-QNM) in environmental conditions. The measurements were realized between tungsten spherical particles with different sizes glued onto tip-less CP-FM (Colloidal Probe for Force Modulation) cantilevers and three different tungsten surfaces with various roughnesses. Samples were cleaned by successive ultrasonic baths of acetone and ethanol and dried before being mounted in the AFM. For each particle/surface configuration, an AFM topographic image (see Figure 5-a) with a minimum size of 10 x 10 μm^2 composed of a matrix of 128 x 128 points with a scanning rate of 0.1 Hz has been realized. A force/distance curve can thus be obtained for each pixel of the adhesion image. An adhesion force distribution is then extracted from the adhesion image (Figure 5-b) and approximated with log-normal distribution as shown in Figure 5(c).

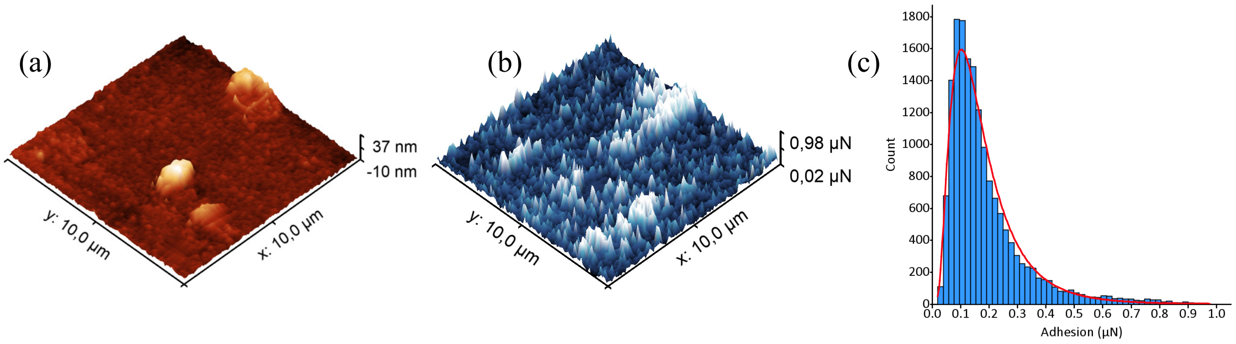

Figure 5: (a) Topographic AFM image (10 x 10 μm^2) obtained in PF-QNM mode with a 3.9 μm tungsten particle. (b) Adhesion image resulting of the PF-QNM scan and (c) adhesion force distribution extracted from the AFM force image with a 3.9 μm radius tungsten particle. The log-normal fit is described by the red continuous line.

Repeatability has been tested by measuring twice the adhesion force distribution on the same area (10 x 10 μm^2) on a nanoscale tungsten substrate with the same colloidal probe cantilever and same scanning parameters. Mean adhesion force of the two measurements is found identical (0.16 % of difference) and the variation (twice the standard deviation) of each measurement lies around 5 %. For most configurations (particle/substrate), at least three different regions have been scanned thus giving three log-normal adhesion force distributions. The mean and the spread of these log-normal adhesion distributions can be then compared with the adhesion force models. It has to be recalled here that, for each adhesion image, 16384 pull-off force values are obtained giving in a single image a good statistical representation of the distribution of the adhesion between the particle and a specific substrate.

2.2. Materials

Functionalized cantilevers. Tungsten particles were purchased from Tekna Advanced Materials™ which produces metallic powders by a RF plasma discharge technique (see Jiang and Boulos [2006]). The Tekna W25 powder comes with a broad size distribution with spherical particles with radius between 4 μm and 15 μm. In order to perform the grafting of spherical particles with best control, a wet sieving method has been used in order to reduce the broadness of the mean particle size. After this step, batches of powders with narrower particle size distributions were used for functionalization of the cantilevers. For smaller particle radii, i.e. between 1 μm and 4 μm, a specific tungsten powder from Alfa Aesar® with a median radius of 2.2 μm and a geometric standard deviation of 1.6 has been sent to Tekna Advanced Materials™ to undergo the same spheroidization procedure. Tungsten spherical particles of desire sizes were then grafted on AFM tip-less cantilevers using optical microscope, micromanipulator and epoxy following method introduced by Ducker et al. [1991] and well detailed by Gan [2007]. Grafted cantilevers were verified by SEM analysis before and after pull-off force experiments in order to estimate their radii and check that no contamination was present on the particles. Figure 6 shows SEM micrographs of these particles once attached onto AFM cantilevers. Seven particle radii have been investigated in this study: 1 μm, 1.8 μm, 3 μm, 3.9 μm, 5.5 μm, 7.5 μm and 10.5 μm. SEM analysis also emphasized that no plastic deformations were visible after pull-off force experiments. The spring constant of the functionalized cantilevers was measured using the Thermal Tune method provided by the Bruker AFM software. The thermal method calibrates the spring constant of a cantilever by fitting the power spectral density of the cantilever fluctuations with a known Lorentzian curve. The calibration procedure has been repeated three times for each cantilever in order to have the variation of the spring constant. Note that tungsten spherical particles were added to the cantilevers before spring constants were determined. The radii of the tungsten spheres and the corresponding spring constants of the cantilevers are provided in Table 1.

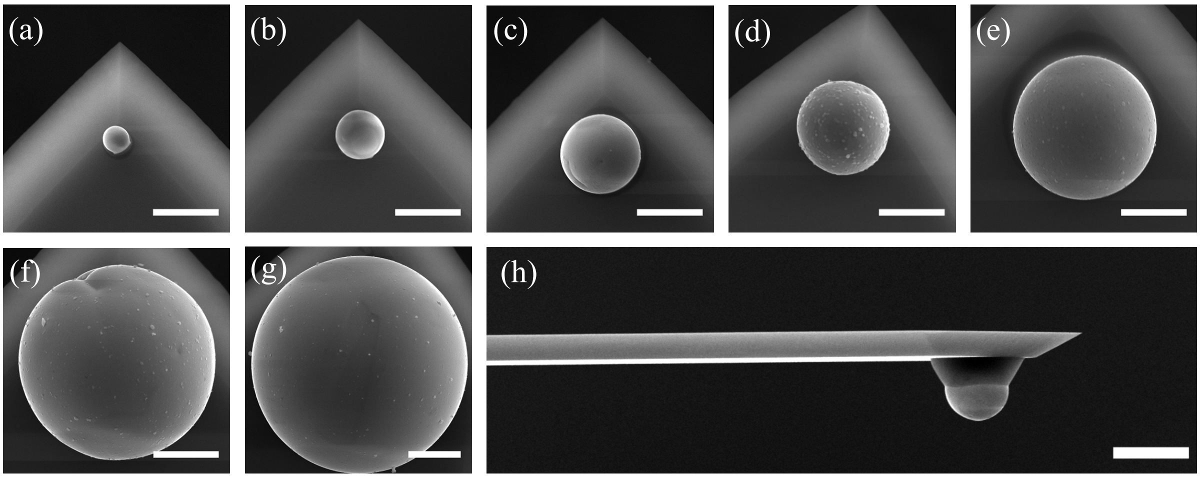

Figure 6: SEM micrographs of tungsten spherical particles grafted onto tip-less cantilevers. Sphere radii are (a) 1 μm, (b) 1.8 μm, (c) 3 μm, (d) 3.9 μm, (e) 5.5 μm, (f) 7.5 μm and (g) 10.5 μm. Side view of the 3.9 μm sphere (h) is also presented. Scale bars are 10 μm in length.

Table 1: Radii of tungsten spheres attached to the cantilevers measured by SEM and spring constants of the cantilevers with particles attached.

réf. Figure 6	(a)	(b)	(c)	(d)	(e)	(f)	(g)
Particle radius (μm)	1 ± 0.05	1.8 ± 0.05	3 ± 0.05	3.9 ± 0.1	5.5 ± 0.1	7.5 ± 0.1	10.5 ± 0.1
Spring constant (N/m)	2.53 ± 0.04	2.69 ± 0.03	2.22 ± 0.12	1.92 ± 0.06	1.89 ± 0.11	2.29 ± 0.16	3.03 ± 0.18

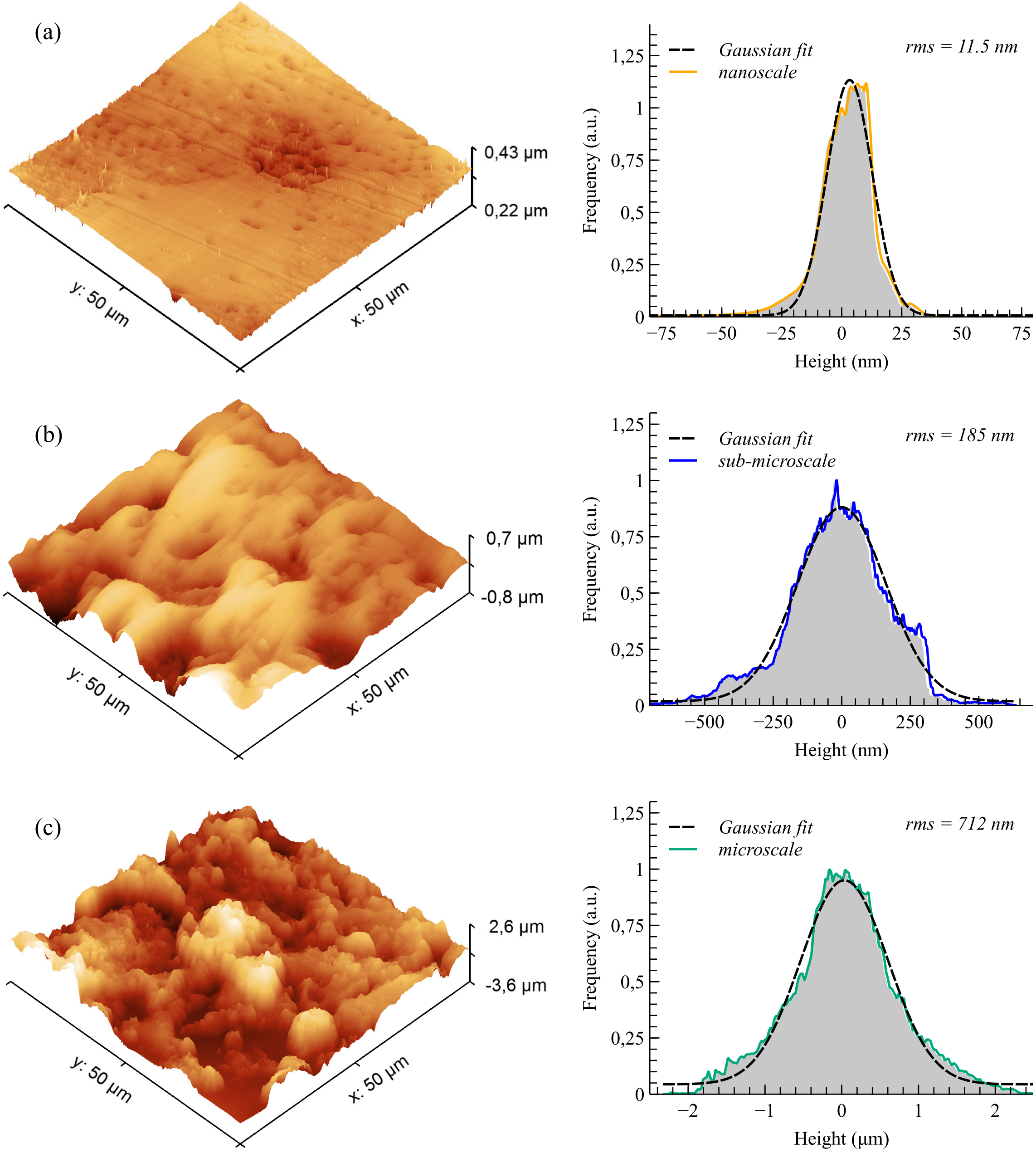

Figure 7: AFM three-dimensional images (50 x 50 μm^2) of (a) the nanoscale tungsten surface, (b) the sub-microscale tungsten surface and (c) the microscale tungsten surface used in the pull-off force measurements. Height histograms of the three substrates are represented together with Gaussian fits (discontinuous black lines).

Surface characterization. Three tungsten surfaces with different roughnesses and textures have been used in this study. Two bulk tungsten substrates were polished in order to reach specific roughness. The first one has been mirror polished using different grades of SiC papers and diamond paste to reach a *rms* surface roughness of the order 10 nm. It will be referred as nanoscale tungsten substrate in the following. The second one has been hand-polished and exhibits a *rms* surface roughness in the range $100 - 200$ nm (referred as sub-microscale surface in the following). The third tungsten substrate has been exposed to high temperatures (above 1000 °C) by He plasma using radiofrequence (RF) hollow cathode discharge technique described by Stancu et al. [2017] (referred as microscale surface in the following). The dimensions of the tungsten substrates are approximately $5 \times 5\ mm^2$. AFM topographic measurements in ScanAsyst mode (Bruker) with standard Scanasyst probes have been performed on the three surfaces and are depicted in Figure 7. The scans are $50 \times 50\ \mu m$ in size with a resolution of 2048×2048 data points. Height histograms of the three substrates are represented in Figure 7 together with Gaussian fits that permits to calculate the *rms* roughnesses (standard deviation of the height distributions) of each substrate. The root-mean-square roughness (also referred as R_q) is defined by:

$$R_q = \sqrt{\frac{1}{MN}\sum_{i=1}^{M}\sum_{j=1}^{N}(z(i,j))^2}, \tag{8}$$

with $M \times N$ a matrix containing the height data $z(i, j)$. The calculated roughnesses (R_q) are 11.5 nm, 185 nm and 712 nm for the nanoscale surface, the sub-microscale surface and the microscale surface respectively.

3. Results and Discussion

3.1. Estimation of the Hamaker constant

In this section we present the method we used to measure the Hamaker constant for W/W interaction in ambient air. The cantilever with the grafted 10.5 μm radius particle has been used to performed pull-off measurements in 20 different locations on the nanoscale W substrate. For this particular measurement, simple force-distance curves where obtained and analyzed in each location. Using the classical expression of van der Waals forces given by Eq. (1) and taking the closest distance $z_0 = 0.45$ nm, we found an average Hamaker constant of $19.9 \pm 2 \times 10^{-20}$ J which is two times below the theoretical values of A_H calculated using Lifshitz theory, i.e. $40 - 50 \times 10^{-20}$ J (Tolias [2018]). The low values obtained experimentally can be explained by the influence of roughness of both contacting surfaces. Indeed, the nanoscale tungsten substrate exhibits a nanoscale roughness of 11.5 nm. Identically, the tungsten particle possesses its own surface roughness that we have calculated after mapping the top of the particle with AFM tapping mode (image dimension of $2 \times 2\ \mu m^2$). Figure 8 depicts a 2 μm wide line profile extracted from the AFM topography image taken at the top of the 10.5 μm particle. By substituting the fit parabola (red line in Figure 8) to the measured profile (blue line), we are able to plot the equivalent roughness that would be measured on a flat surface. In this case, the W particle shows a sub-nanoscale structured surface with a *rms* roughness of 0.29 nm.

Although such atomic-scale roughness has proved to reduce adhesion by nearly an order of magnitude compared to atomically flat surface (Jacobs et al. [2013]), in the present interaction the separation distance between the colloidal

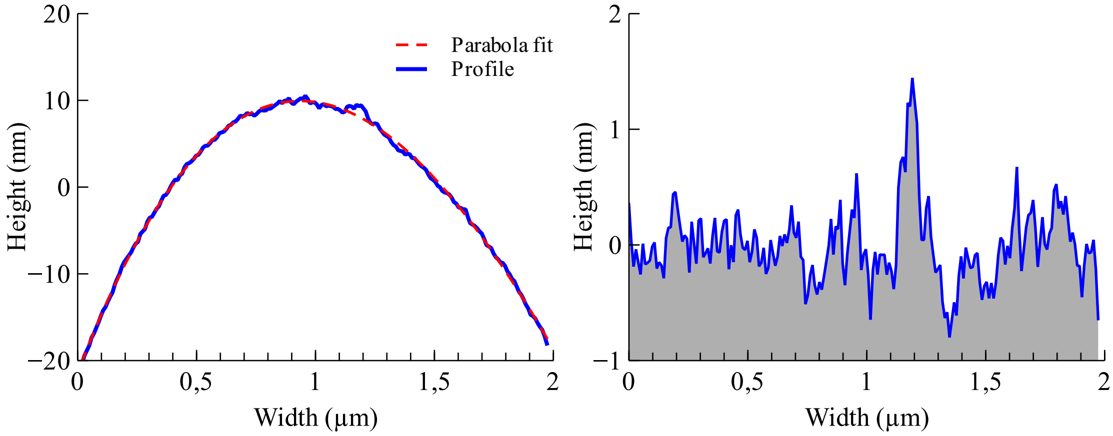

Figure 8: (top) Line profile at the top of the 10.5 μm particle (blue line) and parabola fit (red line). (bottom) Roughness profile of the top of the particle after removal of the parabolic fit.

probe and the substrate is governed by the nanoscale roughness of the latter. In order to account for the roughness effect in the calculation of the Hamaker constant, we use the classical formula of the Rabinovich model presented in section I of this paper:

$$A_{exp} = \frac{6 \cdot F_{exp} \cdot z_0^2}{R_p} \left[\frac{1}{1 + 58\text{rms}_2 R_p/\lambda_2^2} + \frac{1}{\left(1 + 58\text{rms}_1 R_p/\lambda_1^2\right)(1 + 1.82\text{rms}_2/z_0)^2} \right]^{-1} . \tag{9}$$

The experimental Hamaker constants obtained with the classical formula of Hamaker and the Rabinovich model taking into account nanoscale roughness are plotted in Figure 9. The average experimental Hamaker constant obtained when taking into account the nanoscale roughness of the substrate is 37 ± 3.5 × 10^{-20} J. As can be seen from Figure 9, the adhesion measurements are consistent and repeatable with a fluctuation of 10 % over all the measured data.

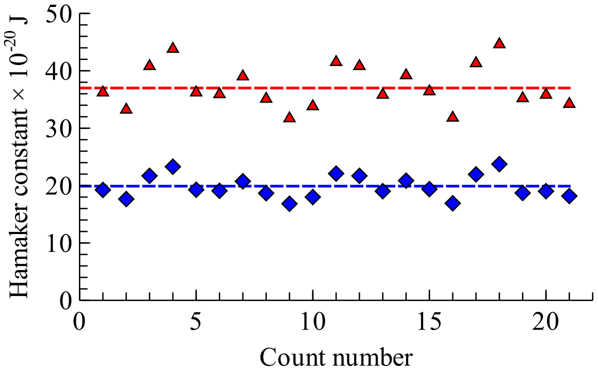

Figure 9: Measured Hamaker constant using a tungsten spherical particle of 10.5 μm radius and nanoscale tungsten surface with the classical formula of Hamaker (blue diamonds) and the model of Rabinovich with roughness correction (red triangles).

The experimental values of Hamaker constant obtained with pull-off force data and adjusted with the Rabinovich model are in good agreement with the theoretical value of Hamaker constant for W/W interaction considering the experimental conditions (measurements were performed in ambient air) and the repeatability of the technique. Moreover, it is worth mentioning that pure tungsten is not chemically stable in ambient conditions and it is well known that a thin WO_3 oxide layer ($\approx 3-6$ nm) forms at the surface of tungsten material (see Peillon et al. [2017]). Such an oxide layer adds to the complexity of the measurement for a pure W/W adhesion study and the determination of van der Waals interaction by modifying the Hamaker constant of the material. Nevertheless, since all the force measurements presented in this paper were realized in ambient air, we will consider an Hamaker constant of $A_{exp} = 37 \pm 3.5 \times 10^{-20}$ J in the following.

3.2. *Comparison with the Rabinovich model*

We present in this section the mean and standard deviation parameters of the adhesion force distributions obtained for each particle size and the three different tungsten substrates. Measurements and the outcome of the Rabinovich model are plotted in Figures 10, 11 and 12 using the surface parameters given in table 2. These parameters where extracted from AFM topography measurements presented in Figure 7.

Table 2: Surface parameters (in nm) used with the Rabinovich model

Samples	λ_1	rms_1	λ_2	rms_2
nanoscale	2780	9.6	1500	3.2
sub-microscale	12800	130	650	21
microscale	2130	717	300	27

Derivations of adhesion forces with the Rabinovich model were performed with a minimal separation distance $z_0 = 0.45$ nm and the experimental Hamaker constant estimated previously $A_{exp} = 37 \times 10^{-20}$ J and are represented by the continuous lines in Figures 10, 11 and 12. We also performed the calculations of adhesion forces with the minimum ($A_{min} = 33.5 \times 10^{-20}$ J) and maximum ($A_{max} = 40.5 \times 10^{-20}$ J) Hamaker constants deduced from the measurement in Section 3.1. These limit values are denoted $A_{\pm 10\%}$ and are depicted by the dashed lines in Figures 10, 11 and 12.

Tungsten surface with nanoscale roughness. Adhesion measurements obtained with the nanoscale tungsten surface are presented in Figure 10 together with the Rabinovich model derivations.

Experimental adhesion measurements on the nanoscale roughness tungsten surface with tungsten particles from 1 μm to 10.5 μm radius exhibit mean adhesion forces between 300 nN and 1700 nN. Standard deviations of the mean adhesion forces are below 5 % except for the 3.9 μm radius particle and the larger 10.5 μm radius particle where the standard deviations are 22 % and 10 % respectively. In comparison, the classical Hamaker formula for the derivation of the van der Waals force (eq. 1) between a sphere and a plane gives 3 350 nN for the 10.5 μm radius particle which is two times the experimental value. This two times overestimate by the model is clearly related to the surface roughness. This is confirmed by Figure 10 where the Rabinovich model is consistent with data for all particle sizes tested except for the 3.9 μm particle radius.

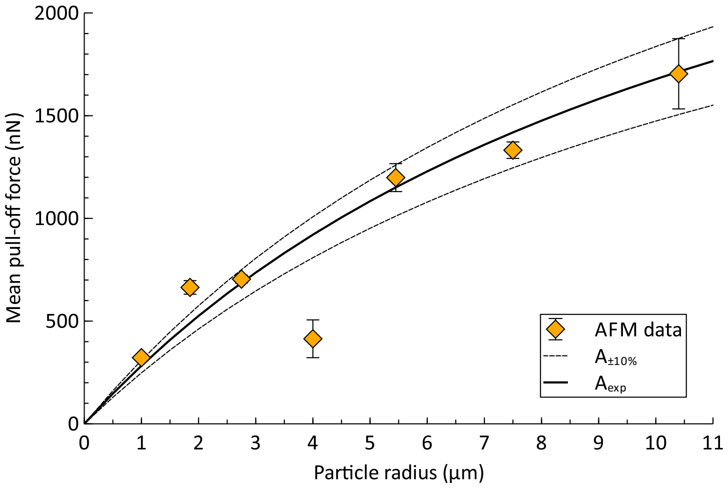

Figure 10: Mean adhesion forces versus particle radius with the nanoscale tungsten surface. Continuous and dashed lines represent the Rabinovich model derivations with the experimental Hamaker constant A_{exp} and its 10% variation.

Effect of particle roughness. Indeed, the experimental mean adhesion force with the 3.9 μm particle radius is 414 nN which is two times lower than the predicted adhesion by the Rabinovich model. Such a drop in the adhesion can again be explained by the surface roughness of the particle itself. To confirm this hypothesis, we measured the topography of the summit of this particle with the AFM. A nanostructured surface was found with a *rms* of 12.6 nm. Such an important roughness cannot be ignored and have to be incorporated in the Rabinovich derivation. To do so, we simplified the problem by considering that the roughness of the particle rms_p adds-up to the superimposed nanoscale roughness rms_2 of the substrate. We can thus rewrite the superimposed roughness used by the Rabinovich model as follows: $rms_3 = \sqrt{rms_p^2 + rms_2^2}$ which gives 13 nm. With this new roughness value, the derivation of the adhesion force for the 3.9 μm particle radius gives 440 nN which is much closer to the observed experimental value considering the variations observed ($\approx$ 10%). On the other hand, derivations using the modified Rumpf model (eq. 2) and the same parameters (i.e. closest distance between surfaces z_0 and Hamaker constant A_{exp}) were carried out with the *rms* roughness of 11.5 nm and returned adhesion values between 10 nN and 30 nN which are far from experimental data. As discussed previously in Figure 2, the minimal value of normalized adhesion forces for micron-sized particles predicted by the modified Rumpf model occurs precisely for *rms* roughness close to 10 nm. For such a range of roughness, we show that the modified Rumpf model greatly underestimate adhesion forces and should not be used in that case.

Tungsten surface with sub-microscale roughness. Adhesion measurements obtained with the sub-microscale tungsten surface are presented in Figure 11 together with the Rabinovich and Rumpf model calculations.

Experimental adhesion measurements on the tungsten sub-microscale roughness surface with tungsten particles from 1 μm to 10.5 μm radius exhibit mean adhesion forces between 10 nN and 115 nN which is one order of magnitude below data obtained with the tungsten nanoscale surface. On the other hand, the standard deviations of the mean

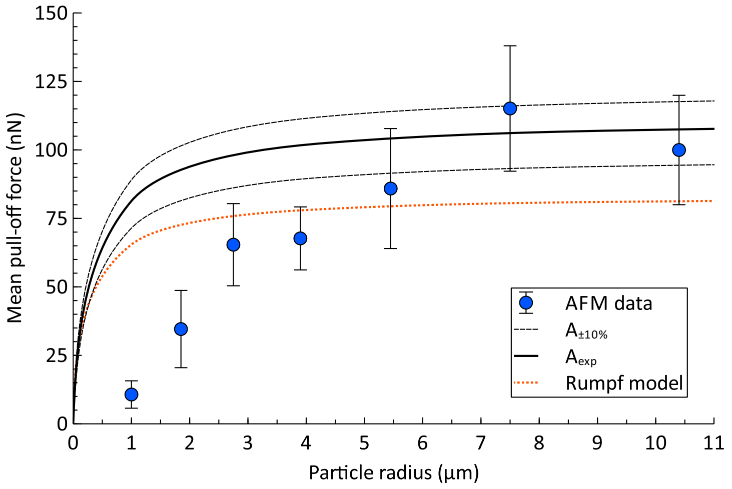

Figure 11: Mean adhesion forces versus particle radius with the sub-microscale tungsten surface. Continuous and dashed lines represent the Rabinovich model derivations with the experimental Hamaker constant A_{exp} and its 10% variation.

adhesion forces are much larger with values between 19 % and 46 %. Rabinovich model is consistent with data for particle above 5.5 μm in radius but fails to describe the adhesion reduction observed when the particle radius is below 5 μm. This specific feature remains unexplained. Using the same parameters and the *rms* roughness of 185 nm for the sub-microscale tungsten surface, we plotted the modified Rumpf model calculations in Figure 11. In this case, results are of same order of magnitude with experimental data. However, the Rumpf model still underestimate by 25 % the adhesion forces compared to Rabinovich derivations.

Tungsten surface with microscale roughness. Adhesion measurements obtained with the microscale tungsten surface are presented in Figure 12 together with the Rabinovich model calculations.

Experimental adhesion measurements on the microscale roughness tungsten surface with tungsten particles from 1 μm to 10.5 μm radius exhibit mean adhesion forces between 10 nN and 30 nN. Standard deviations of the mean adhesion forces are consequent and above 80 % for all the mean adhesion forces. In such a case with a very textured substrate composed of a microscale roughness, adhesion of micrometer particles becomes independent with the particle size as previously noticed by Laitinen et al. [2013]. In this case, surface roughness appears to play the dominant role whereas particle size has a secondary influence on adhesion force. This behavior is well described by the Rabinovich model which returns values that are the same order of magnitude than experimental data. In contrast, derivations using the modified Rumpf model with the *rms* roughness of 712 nm returned adhesion values between 103 nN and 293 nN which are one order of magnitude higher than experimental data.

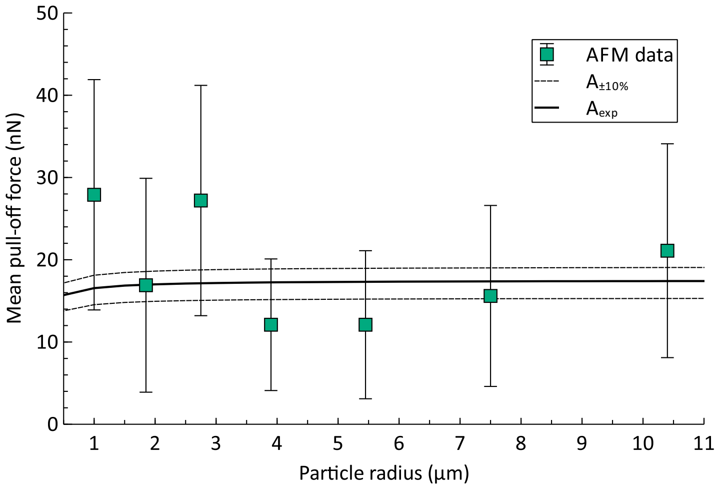

Figure 12: Mean adhesion forces versus particle radius with the microscale tungsten surface. Continuous and dashed lines represent the Rabinovich model derivations with the experimental Hamaker constant A_{exp} and its 10% variation.

4. Conclusion

Adhesion forces between tungsten spherical microparticles with radii from 1 μm to 10.5 μm and tungsten substrates with different roughnesses have been measured in ambient air using the Atomic Force Microscopy (AFM) colloidal probe technique. Mean roughnesses of the tungsten substrates were measured by AFM and were ranked in three categories i.e. nanoscale, sub-microscale and microscale roughnesses. Experimental Hamaker constant of $37 \pm 3.5 \times 10^{-20}$ J has been obtained using a spherical tungsten particle of 10.5 μm in radius and a tungsten substrate with nanoscale root-mean-square roughness of $rms = 11.5$ nm. Pull-off force measurements with a nanoscale tungsten substrate (nanoscale rms) and microparticles with radii from 1 μm to 10.5 μm gave adhesion forces in the range 300 nN to 1700 nN. On the other hand, it was shown that larger roughness in the micrometer range induces a two orders of magnitude decrease on the adhesion of the tungsten microparticles compared to the tungsten surface with nanoscale roughness. Sub-micrometer surface roughness ($rms = 185$ nm) exhibited adhesion forces in the range 10 nN to 115 nN in accordance with both the Rabinovich and the Rumpf models. Moreover, we have also shown that:

- Comparison with the van der Waals-based adhesion force model of Rabinovich showed quantitative agreement with experimental pull-off forces for particles with radii between 1 μm and 10.5 μm for smooth surfaces ($rms \approx$ 10 nm) but also for very rough substrates with a rms roughness close to the micrometer range.
- For all the configurations tested, we demonstrated the predictive accuracy of the Rabinovich model when definition of the surface roughness is carried out with care.
- For microscale roughness, measurements have shown that dependency of adhesion force with particle size (in the micrometer range) has a secondary influence compared to the roughness of surfaces.

The good predictions of the Rabinovich model throughout the range of micron-sized particles and *rms* roughnesses studied makes it a good substitute to classical empirical correlations (for example the correlation of Biasi [2001]) used in common resuspension models like the Rock'n roll model of Reeks and Hall [2001] by placing the roughness of the substrate on which particles are deposited as a key parameter for removal predictions as recently stated by Henry and Minier [2018]. When available, experimental adhesion force distributions obtained by AFM can replace mathematical description of adhesion forces used in numerical codes for resuspension predictions like in Guingo and Minier [2008], Benito et al. [2015]. Such combination between adhesion force distribution measured by AFM colloidal probe technique and a resuspension model is intended to be tested by the authors in a future work.

Acknowledgments

This work has been carried out within the framework of the EUROfusion Consortium and has received funding under grant number AWP17-ENR-MFE-CEA-10. The views and opinions expressed herein do not necessarily reflect those of the European Commission. The authors thank L.O Heim from SQUBE Company (Germany) for the grafting of particles onto cantilevers.

Benito, J., Aracena, K., Uñac, R., Vidales, A., and Ippolito, I. (2015). Monte Carlo modelling of particle resuspension on a flat surface. *Journal of Aerosol Science*, 79:126–139.

Biasi, L. (2001). Use of a simple model for the interpretation of experimental data on particle resuspension in turbulent #ows. *Aerosol Science*, page 26.

Brambilla, S., Speckart, S., and Brown, M. J. (2017). Adhesion and aerodynamic forces for the resuspension of non-spherical particles in outdoor environments. *Journal of Aerosol Science*, 112:52–67.

Butt, H.-J., Cappella, B., and Kappl, M. (2005). Force measurements with the atomic force microscope: Technique, interpretation and applications. *Surface Science Reports*, 59(1-6):1–152.

Cho, A. Y. H. (1964). Contact Charging of Micron-Sized Particles in Intense Electric Fields. *Journal of Applied Physics*, 35(9):2561–2564.

Cooper, D. W., Wolfe, H. L., and Miller, R. J. (1988). Electrostatic Rremoval of particles from surfaces. In *Particles on Surfaces 1*, Plenum Press, page 11. K. L. Mittal (éd.), New York.

Derjaguin, B., Muller, V., and Toporov, Y. (1975). Effect of contact deformations on the adhesion of particles. *Journal of Colloid and Interface Science*, 53(2):13.

Ducker, W. A., Senden, T. J., and Pashley, R. M. (1991). Direct measurement of colloidal forces using an atomic force microscope. *Nature*, 353:239–241.

Fuller, K. N. G. and Tabor, D. (1975). The Effect of Surface Roughness on the Adhesion of Elastic Solids. *Proceedings of the Royal Society A: Mathematical, Physical and Engineering Sciences*, 345(1642):327–342.

Gan, Y. (2007). Invited Review Article: A review of techniques for attaching micro- and nanoparticles to a probe's tip for surface force and near-field optical measurements. *Review of Scientific Instruments*, 78(8):081101.

Gauthier, e., Alvo, e., Dejeu, o., Tamadazte, B., Rougeot, P., and Regnier (2013). Analysis and Specificities of Adhesive Forces Between Microscale and Nanoscale. *IEEE Transactions on Automation Science and Engineering*, 10(3):562–570.

Guingo, M. and Minier, J.-P. (2008). A new model for the simulation of particle resuspension by turbulent flows based on a stochastic description of wall roughness and adhesion forces. *Journal of Aerosol Science*, 39(11):957–973.

Götzinger, M. and Peukert, W. (2003). Dispersive forces of particle–surface interactions: direct AFM measurements and modelling. *Powder Technology*, 130(1-3):102–109.

Götzinger, M. and Peukert, W. (2004). Particle Adhesion Force Distributions on Rough Surfaces. *Langmuir*, 20(13):5298–5303.

Hamaker, H. (1937). The London—van der Waals attraction between spherical particles. *Physica*, 4(10):1058–1072.

Heim, L. O., Ecke, S., Preuss, M., and Butt, H.-J. (2002). Adhesion forces between individual gold and polystyrene particles. *Journal of Adhesion Science and Technology*, 16(7):829–843.

Henry, C. and Minier, J.-P. (2018). Colloidal particle resuspension: On the need for refined characterisation of surface roughness. *Journal of Aerosol Science*, 118:1–13.

Israelachvili, J. N. (2011). *Intermolecular and Surface Forces*. Academic Press.

Jacobs, T. D. B., Ryan, K. E., Keating, P. L., Grierson, D. S., Lefever, J. A., Turner, K. T., Harrison, J. A., and Carpick, R. W. (2013). The Effect of Atomic-Scale Roughness on the Adhesion of Nanoscale Asperities: A Combined Simulation and Experimental Investigation. *Tribology Letters*, 50(1):81–93.

Jiang, X.-L. and Boulos, M. (2006). Induction plasma spheroidization of tungsten and molybdenum powders. *Transactions of Nonferrous Metals Society of China*, 16(1):13–17.

Johnson, K. L., Kendall, K., and Roberts, A. D. (1971). Surface energy and the contact of elastic solids. *Proceedings of the Royal Society A: Mathematical, Physical and Engineering Sciences*, 324:301–313.

Jones, R., Pollock, H. M., Cleaver, J. A. S., and Hodges, C. S. (2002). Adhesion Forces between Glass and Silicon Surfaces in Air Studied by AFM: Effects of Relative Humidity, Particle Size, Roughness, and Surface Treatment. *Langmuir*, 18(21):8045–8055.

Krasheninnikov, S. I., Smirnov, R. D., and Rudakov, D. L. (2011). Dust in magnetic fusion devices. *Plasma Physics and Controlled Fusion*, 53(8):083001.

Krupp, H. (1967). Particle adhesion: theory and experiment. *Adv. Colloid Interface Sci.*, 1:111_239.

Laitinen, O., Bauer, K., Niinimäki, J., and Peuker, U. (2013). Validity of the Rumpf and the Rabinovich adhesion force models for alumina substrates with nanoscale roughness. *Powder Technology*, 246:545–552.

LaMarche, C. Q., Leadley, S., Liu, P., Kellogg, K. M., and Hrenya, C. M. (2017). Method of quantifying surface roughness for accurate adhesive force predictions. *Chemical Engineering Science*, 158:140–153.

Leite, F. L., Bueno, C. C., Da Róz, A. L., Ziemath, E. C., and Oliveira, O. N. (2012). Theoretical Models for Surface Forces and Adhesion and Their Measurement Using Atomic Force Microscopy. *International Journal of Molecular Sciences*, 13(12):12773–12856.

Matsusaka, S. and Masuda, H. (1996). Particle Reentrainment from a Fine Powder Layer in a Turbulent Air Flow. *Aerosol Science and Technology*, 24(2):69–84.

Maugis, D. (1992). Adhesion of spheres: The JKR-DMT transition using a dugdale model. *Journal of Colloid and Interface Science*, 150(1):243–269.

Mizes, H., Ott, M., Eklund, E., and Hays, D. (2000). Small particle adhesion: measurement and control. *Colloids and Surfaces A: Physicochemical and Engineering Aspects*, 165(1-3):11–23.

Mokgalapa, N. M., Ghosh, T. K., and Loyalka, S. K. (2014). Graphite Particle Adhesion to Hastelloy X: Measurements of the Adhesive Force with an Atomic Force Microscope. *Nuclear Technology*, 186(1):45–59.

Olsson, L., Tengvall, P., Wigren, R., and Erlandsson, R. (1992). Interaction forces between a tungsten tip and methylated SiO2 surfaces studied with scanning force microscopy. *Ultramicroscopy*, 42-44:73–79.

Parsegian, V. A. (2005). *Van der Waals Forces: A Handbook for Biologists, Chemists, Engineers, and Physicists*. Cambridge University Press, Cambridge.

Peillon, S., Roynette, A., Grisolia, C., and Gensdarmes, F. (2014). Resuspension of carbon dust collected in Tore Supra and exposed to turbulent airflow: Controlled experiments and comparison with model. *Fusion Engineering and Design*, 89(11):2789–2796.

Peillon, S., Sow, M., Grisolia, C., Miserque, F., and Gensdarmes, F. (2017). Mobilization of tungsten dust by electric forces and its bearing on tritiated particles in the ITER tokamak. *Journal of Electrostatics*, 88:111–115.

Petean, P. and Aguiar, M. (2015). Determining the adhesion force between particles and rough surfaces. *Powder Technology*, 274:67–76.

Rabinovich, Y. I., Adler, J. J., Ata, A., Singh, R. K., and Moudgil, B. M. (2000a). Adhesion between Nanoscale Rough Surfaces : measurements and comparison with theory. *Journal of Colloid and Interface Science*, 232(1):17–24.

Rabinovich, Y. I., Adler, J. J., Ata, A., Singh, R. K., and Moudgil, B. M. (2000b). Adhesion between Nanoscale Rough Surfaces : Role of asperity geometry. *Journal of Colloid and Interface Science*, 232(1):10–16.

Reeks, M. W. and Hall, D. (2001). Kinetic models for particle resuspension in turbulent #ows: theory and measurement. *Aerosol Science*, page 31.

Ripperger, S. and Hein, K. (2004). Measurement of Adhesion Forces between Particles and Rough Substrates in Air with the Vibration Method. *KONA Powder and Particle Journal*, 22(0):121–133.

Riva, G., Tolias, P., Ratynskaia, S., Daminelli, G., Donde, R., De Angeli, M., Vassallo, E., and Pedroni, M. (2017). Adhesion measurements for tungsten dust deposited on tungsten surfaces. *Nuclear Materials and Energy*, 12:593–598.

Rondeau, A., Peillon, S., Roynette, A., Sabroux, J.-C., Gelain, T., Gensdarmes, F., Rohde, V., Grisolia, C., and Chassefière, E. (2015). Characterization of dust particles produced in an all-tungsten wall tokamak and potentially mobilized by airflow. *Journal of Nuclear Materials*, 463:873–876.

Rumpf, H. (1990). *Particle technology*. Chapman and Hall, London. OCLC: 472909018.

Salazar-Banda, G., Felicetti, M., Gonçalves, J., Coury, J., and Aguiar, M. (2007). Determination of the adhesion force between particles and a flat surface, using the centrifuge technique. *Powder Technology*, 173(2):107–117.

Stancu, C., Stokker-Cheregi, F., Moldovan, A., Dinescu, M., Grisolia, C., and Dinescu, G. (2017). Modification of W surfaces by exposure to hollow cathode plasmas. *Applied Physics A*, 123(10).

Szarek, T. R. and Dunn, P. F. (2007). An Apparatus to Determine the Pull-Off Force of a Conducting Microparticle from a Charged Surface. *Aerosol Science and Technology*, 41(1):43–50.

Takeuchi, M. (2006). Adhesion forces of charged particles. *Chemical Engineering Science*, 61(7):2279–2289.

Tolias, P. (2018). Lifshitz calculations of Hamaker constants for fusion relevant materials. *Fusion Engineering and Design*, 133:110–116.

Tolias, P., Riva, G., De Angeli, M., Ratynskaia, S., Daminelli, G., Lungu, C., and Porosnicu, C. (2018). Adhesive force distributions for tungsten dust deposited on bulk tungsten and beryllium-coated tungsten surfaces. *Nuclear Materials and Energy*, 15:55–63.

Wanka, S., Kappl, M., Wolkenhauer, M., and Butt, H.-J. (2013). Measuring Adhesion Forces in Powder Collectives by Inertial Detachment. *Langmuir*, 29(52):16075–16083.

Xie, H. (1997). The role of interparticle forces in the fluidization of fine particles. *Powder Technology*, 94(2):99–108.

Zafar, U., Hare, C., Hassanpour, A., and Ghadiri, M. (2014). Drop test: A new method to measure the particle adhesion force. *Powder Technology*, 264:236–241.

Zhang, T., Peng, W., Shen, K., and Yu, S. (2015). AFM measurements of adhesive forces between carbonaceous particles and the substrates. *Nuclear Engineering and Design*, 293:87–96.